E-ISSN: 2717-2937 | P-ISSN: 2783-1337

International Journal of Research in Industrial Engineering

www.riejournal.com

Int. J. Res. Ind. Eng. Vol. 12, No. 1 (2023) 43–52.

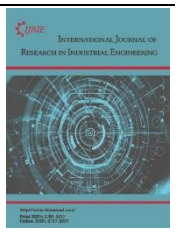

Paper Type: Research Paper

Prediction of Stress Concentration Factor in Butt Welding Joints Using Artificial Neural Networks

Alper Kiraz[1,*], Enes Furkan Erkan[1], Onur Canpolat[1], Onur Kökümer[2]

[1] Department of Industrial Engineering, Sakarya, Turkey; kiraz@sakarya.edu.tr; eneserkan@sakarya.edu.tr; onurcanpolat@sakarya.edu.tr.
[2] Aspen Construction and Floor Systems Industry and Trade Inc., Sakarya, Turkey; onur.kokumer@aspen.com.tr.

Citation:

Kiraz, A., Furkan Erkan, E., Canpolat, O., & Kökümer, O. (2023). Prediction of stress concentration factor in butt welding joints using artificial neural networks. *International journal of research in industrial engineering, 12*(1), 43-52.

Received: 01/07/2022 Reviewed: 02/08/2022 Revised: 22/10/2022 Accepted: 01/12/2021

Abstract

In welded constructions, there should be no defects in the welding seams, or defects should have in an acceptable range for obtaining more reliable welding operations. An undercut is one of the most important welding defects occurring on the workpieces produced by butt welding. Determining the correct value of the Stress Concentration Factor (SCF) allows deciding whether it accepts welding defects, in which case. Many characteristics and ranges influence SCF, making it challenging to calculate a more precise SCF. In this study, six different Artificial Neural Networks (ANNs) models are developed for predicting SCF. These models differ in terms of the training dataset used (70%-90%) and the number of neurons (5-10-20) in the hidden layer. Developed ANN models consist of three input variables the ratio of Undercut depth (h) and Undercut deep Radius (r), reinforcement angle (Q1), deep angle of welding seam (Q2), and an output variable as SCF. The prediction performance of 6 developed ANN models in different specifications is compared. The model with a 90% training set and five neurons in the hidden layer performed the best with an accuracy of 0.9834. According to the ANN model with these features, MAE, MAPE, and RMSE values are calculated as 0.0094, 2.50%, and 0.0129, respectively.

Keywords: Welding defects, Stress concentration factor, Artificial neural networks.

1 | Introduction

Welding operation is extensively used in almost every engineering structure, such as air vehicles, marine vehicles, ships, bridges, automobiles, buses, the piping industry, and pressure tanks [1]. Flexion, tension, and integrated fatigue loads, which cause the growth of cracks-like defects, generally affect welded connections. Defects common in welded joints can be classified as low diffusion of the weld, gas pores, undercutting at the weld toe, etc. Therefore, defects give rise to stress concentrations by the crack-like. The defects are usually placed at the weld toe [2]. Besides, residual stresses can occur in welded joints due to discordant thermal strains caused by increasing and decreasing temperature cycles. These stresses, called fatigue, also negatively affect the life of welded structures. Tensile residual stress of yield strength is located at the weld toe regions [3].

One of the most common welding faults caused by stress is undercutting. Defining the Stress Concentration Factor (SCF) is an essential milestone in the fatigue failure analysis of structures. The

Corresponding Author: kiraz@sakarya.edu.tr
https://doi.org/10.22105/riej.2023.349647.1322

findings revealed that SCF and its associated factor, the fatigue notch factor (Kf), significantly impact the analyses. One of the results of stress concentration in welded components is weld discontinuities. Weld geometry parameters such as weld flank angle, weld throat, and weld toe radius also affect stress concentration [4].

While reviewing the literature, numerical and experimental studies are handled together and separately, as shown in the literature summary table (*Table 1*). In addition, studies using predictive models such as Artificial Neural Networks (ANNs), support vector machines, regression methods, Lagrangian interpolation methods, and Bayesian methods are few compared to numerical and experimental studies. In this study, the effect of different training set ratios and different neuron numbers used in the hidden layer on the forecasting performance of ANN, which is a powerful tool in prediction, has been investigated and aimed to fill the gap in the literature and to achieve stronger prediction success.

Table 1. Some studies in literature.

Reference	Year	Material	Method(s)	Prediction Performance	Numerical/ Experimental/ Prediction Model
Guo et al. [5]	2022	High-strength steel wires	Finite element method, Bayesian method	95%	Exp.+Pred.
Abbasnia et al. [6]	2021	Orthotropic plate	A new method based on regression analysis	99%	Num.
Makki et al. [7]	2018	Welded joints	Response surface models	NA	Num.
Li et al. [8]	2020	Cable steel wire	Finite element model	NA	Exp.
Wang et al. [9]	2020	Fillet weld joints	Parametric formula	NA	Num.
Jiang et al. [10]	2018	Multi-planar tubular DT-joints	Parametric equations	More than 80%	Num.
Dabiri et al. [4]	2017	T-welded joint	Neural network	99.99%	Pred.
Bajić et al. [11]	2017	Pipeline	Finite element method, 3D DIC method	NA	Exp.
Wang et al. [12]	2016	Cylindrical pressure vessels	Extreme learning machine	98.73%	Pred.
Ozkan and Toktas [13]	2016	Rectangular plate	Analytical model, regression analysis, finite element analysis, ANN	96.61%	Num.+Exp.+Pred.
Ji et al. [14]	2015	Corrosion pits	The least-squares support vector machine	NA	Pred.
Zappalorto and Carraro [15]	2015	Orthotropic composite plates	Analytical modeling	NA	Num.
Darwish [16]	2012	Isotropic plate with a circular hole	ANSYS parametric design language	94.4%-99.7%	Exp.
Cerit [17]	2013	Circular cylinder	3D stress analyses, torsion formula	NA	Num.+Exp.
Cerit et al. [18]	2010	Butt welded joint	Reinforcement metal in butt welded joint	99%	Num.+Exp.
Arola and Williams [19]	2002	AISI 4130 CR steel	Arola-Ramulu model	98.00%	Num.
Ida and Uemura [20]	1996	Fillet welded joint	Ushirokawas's and Tsuji's formulae	NA	Num.
Chang and Dover [21]	1996	Tubular X and DT joints	Parametric formulae and regression analysis	NA	Num.+Pred.
Guagliano et al. [22]	1993	Crankshaft	Bidimensional model	91.4%-93.1%	Num. + Exp.

Numerical and experimental analyses derive the results of numerous SCF investigations in the literature. There are few AI-supported investigations, and using current mathematical models and conducting

experiments is complex and time-consuming. In addition, the studies have been carried out considering certain values of the parameters and require new analysis and calculations for different parameter values. ANN-based models with high prediction accuracy can process all possible experimental data quickly. The company aims to reduce the number of defects and errors caused by welding. When the stress concentration value in a significant part of the workpiece is exceptionally high, job safety decreases. Controlling the welding seam in welding constructions is critical in this regard. Due to the non-linear relationships between the parameters affecting the SCF value, one of the most effective ways to define SCF is through modeling. To get more effective results and reduce welding errors, a model is developed for SCF.

Numerous experiments are not required to comprehend the correlations between parameters because of the developed ANN model. Because ANN is a technique that does not require any machinery or equipment, numerous experiments, and can generate useful results. ANN is one of the most valuable methods of diversity areas for researchers [23]. Thus, it avoids the need for experimentation, assures that welding faults are identified beforehand, and lowers the rate of defective products, increasing job safety. Recent advancements in the field of ANN technology have helped overcome various issues in engineering procedures. Because of its effective prediction performance, the ANN technique is selecte for the prediction model of the SCF parameter, which is influenced by various parameters [24], [25].

Even when the parameters impacting the SCF value fluctuate, an ANN-based model is built into this work to calculate the SCF value without the requirement for long-term repeating tests. In this study, an ANN-based model was developed to determine the SCF value without requiring time-consuming, repetitive experiments even when the parameters affect the SCF value change. In addition, it has been investigated how constructing the ANN model with different training set ratios and the change in the number of neurons in the hidden layer used in the model is effective in estimating the SCF value.

In summary, the remaining sections of the research cover the following subjects. Section 2 discusses the structure and properties of the ANN model, as well as detailed information regarding SCF. The data is obtained, normalization procedures are performed, and the data is then integrated into the ANN model in Section 3. Then, the prediction performances of six ANN models are evaluated and compared in Section 4. By considering many statistical error types. Finally, the results and findings are included in the conclusions section.

2 | Methodology

2.1 | Stress Concentration Factor

According to experimental results, the stress concentration on welded sections is not uniform. There is no uniformity in manufacturing these elements due to cracks, voids, and other loads. Rarely, occurring stress could be tallied, unlike medial stress (F/A). Also, some sections' stress may be at the highest level. The notch effect occurs when the stress concentration level reaches its maximum value in particular areas, and this difference from the average value causes stress concentration. The change is depicted in *Fig. 1*.

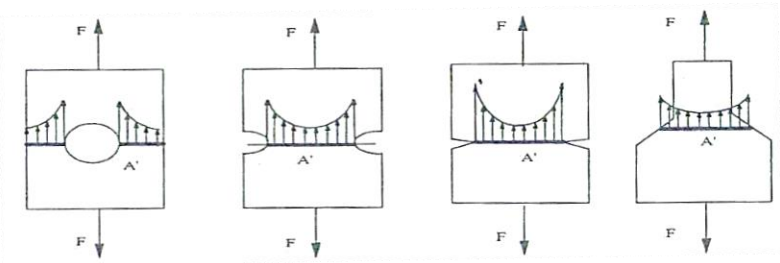

Fig. 1. View of notch sections cause stress concentrations in some tensile conditions.

This situation is calculated mathematically as *Eq. (1)* where σ_{max} describes maximum stress, A' represents the cross-sectional area, and F is force.

$$\sigma_{max} = SCF\frac{F}{A'}. \quad (1)$$

In *Eq. (2)*, the cross-sectional area is stated as A' SCF is a coefficient of total stress loads called SCF. All along SCF value is bigger than 1. So SCF is a ratio of maximum regional stress (σ_{max}) to the average value (σ_{avg}) [7].

$$SCF = \frac{\sigma_{max}}{\sigma_{avg}}. \quad (2)$$

2.2 | Artificial Neural Networks

ANN is a tool that has been developed inspired by neural networks in the human brain and is used to solve complex problems [4]. More than one artificial neuron interacts with each other in a hierarchical structure in ANN [26]. Different elements, such as cells and nodes, exist in this structure, apart from neurons. Some links show the relations of the nodes with each other. Each link has a weight and can be unidirectional or bidirectional. As in the solution algorithms of traditional programming, the step-by-step solution approach is replaced by a neural network structure that searches for a solution by itself according to the predetermined rules in ANN. This neural network structure generates new rules over time and compares the results from these rules with the sample data set results [27].

ANN offers a highly effective estimation for many values, including intermediate values for SCF, saving time and money over performing experiments for every value of each parameter in the input layer. However, the future addition of a new parameter, makes it simpler to analyze its impact. Without this model, numerous experiments would be required to add a single parameter.

ANN is architecturally composed of an input layer, a hidden layer (one or more), and an output layer [28]. The network is tested for the input and output layers. Then, the weights required to give the desired output are calculated. This calculation is called learning. Three different learning methods are used in ANN: supervised learning, unsupervised learning, and reinforcement learning, respectively. The purpose of learning is that the actual and ANN outputs are as close as possible. This value also determines the successful performance of the network.

In general, ANN is divided into feedforward and feedback networks according to the direction of information progression. The input layer, hidden layers, and output layer are in both groups. In feedforward networks, weights establish connections between neurons in the layers. Information moves unidirectionally from the input to the output layer [29]. There is no connection between units in the same layer in feedforward networks. However, neurons are interconnected and have dynamic memory in feedback networks. Due to the context layer in feedback networks, the hidden layer outputs are weighted back to the input layer and re-enter the hidden layer as input. Therefore, information also moves backward in these networks.

The backpropagation algorithm is one of the most used among many different learning algorithms in ANN. The backpropagation algorithm constantly compares the error rates of the actual values in the data set with the output values of ANN and updates the weights. If the output values exceed the desired value, the ANN returns to the previous step by changing the weight values [4].

The input layer, which contains problem-related parameters, gets data processing instructions from another cell or the outside. By summing the multiplication of the information received in the cell (X_1, X_2... X_n) and the weights of the cells (W_1, W_2... W_n), the sum function estimates the cell's net entry information [30]. *Eq. (3)* denotes the sum function where X_i is the value of input criteria and w_i is the weight. *Fig. 2* depicts the structure of ANN.

$$Net = \sum_{i=1}^{n} X_i \cdot w_i. \quad (3)$$

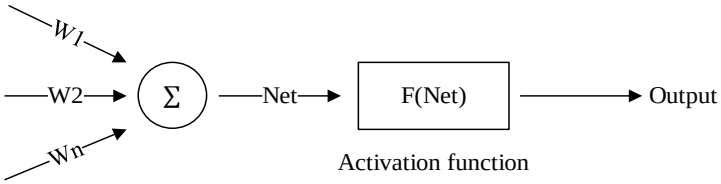

Fig. 2. The structure of ANN.

3 | Implementation

The parameters used in the model are determined within the scope of the study. After the data is obtained using ANSYS mechanical simulation software, data is normalized, and the ANN models are generated. The flow chart of the study is shown in *Fig. 3*.

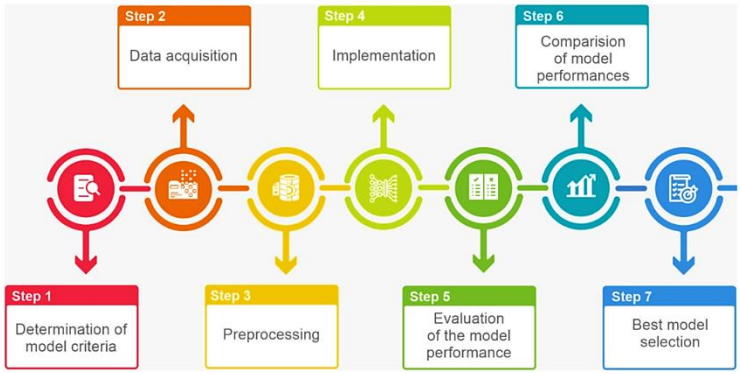

Fig. 3. Flow chart of the study.

3.1 | Data Acquisition

In this study, estimations are handled based on a V-welded workpiece. Undercut defects are common after an arc welding operation. *Fig. 4* shows the parameters that affect the undercut.

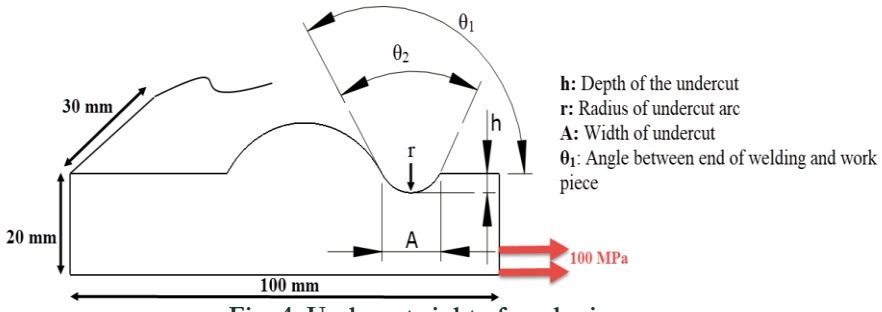

Fig. 4. Undercut sight of work piece.

The pressure value exposed to the workpiece from the front side to the undercut is 100 MPa. According to the parameters below *Table 2*, different workpieces are created as visuals and analyzed to obtain SCF values. A, R, h, and θ_1 are affecting parameters for SCF, and *Table 3* illustrates some of the experimental values for these parameters. These values are calculated using ANSYS Mechanical Simulation Software [18].

Table 2. Parameters of undercut.

h (mm)	θ_1 (degree)	An (mm)	r (mm)
0.5	120	3	0.5
1	140	4	1
1.5	160	5	1.5
2	180		
2.5			

Table 3. Experimental data values.

	h	$\sqrt{h/r}$	$\theta_1 = 180$ SCF	$\theta_1 = 160$	$\theta_1 = 140$	$\theta_1 = 120$
	0.5	1	2.83	3.14	3.3	3.36
	1	1.41	4.41	4.72	4.91	4.94
A:3 R:0.5	1.5	1.73	5.07	5.41	5.5	5.56
	2	2	6.08	6.27	6.34	6.41
	2.5	2.23	7	7.27	7.23	7.31
…	…	…	…	…	…	…
	0.5	0.57	2.04	2.17	2.37	3.48
	1	0.81	2.72	2.85	2.93	2.94
A:5 R:1.5	1.5	1	3.23	3.35	3.41	3.43
	2	1.15	3.74	3.83	3.88	3.89
	2.5	1.28	4.17	4.25	4.29	4.3

The data normalization procedure utilized in ANN effects positively trains the network [31]. As a result, the experimental data are normalized between 0 and 1 using *Eq. (4),* where X is the normalized data, X_i is the experimental data, X_{min} is the minimum value of experimental data and X_{max} is the maximum value of experimental data.

$$X = \frac{X_i - X_{min}}{X_{max} - X_{min}}. \quad (4)$$

3.2 | Developed ANN Models

This study develops six different ANN models for predicting SCF value. The training dataset used (70-90 percent) and the number of neurons in the hidden layer (5-10-20) differ among these models. Developed ANN models consist of three input variables (Undercut depth (h) / Undercut deep Radius (r)), reinforcement angle (Q1), and deep angle of welding seam (Q2), and an output variable as SCF.

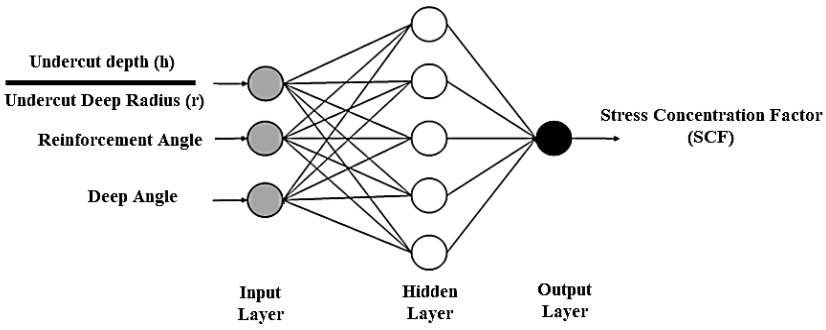

Fig. 5. ANN topology of proposed models.

ANN models have three input layers, a hidden layer, and an output layer, shown in *Fig. 5* as a topology of models. The features of the developed ANN model are given in *Table 4*.

Table 4. Architecture and functions of the implemented ANN.

Network	Feedforward Backpropagation Network
Training function	Levenberg-Marquardt
Learning function	Gradient descent with momentum weights and bias learning function
Transfer function	Tan sigmoid & Linear transfer function
Performance function	Mean squared error
Training dataset rate	70%-90%
Number of neurons in the hidden layer	5-10-20

4 | Statistical Analysis

The prediction performances of the models are compared by calculating MAE, MAPE, RMSE, and R^2 values. According to the results, the prediction performance of the ANN model developed using a training set ratio of 90% and including five neurons in the hidden layer is better. Forecast performances are calculated with the following formulas *Eq. (5-8)* to indicate A_t actual values F_t predicted values. *Table 5* is obtained with the help of the following formulas by comparing the experimental data with the results of the ANN model predictions.

$$MAE = \frac{1}{n}\sum_{t=1}^{n}|A_t - F_t|. \quad (5)$$

$$MAPE = \frac{1}{n}\sum_{t=1}^{n}\frac{|A_t - F_t|}{|A_t|}x100. \quad (6)$$

$$RMSE = \sqrt{\frac{1}{n}\sum_{t=1}^{n}(A_t - F_t)^2}. \quad (7)$$

$$R^2 = 1 - \frac{\sum_{t=1}^{n} A_t - F_t)^2}{\sum_{t=1}^{n}\left(\overline{A_t} - A_t\right)^2}. \quad (8)$$

Table 5. Prediction performance of the models.

Training set ratio	Number of Neurons in the Hidden Layer	MAE	MAPE	RMSE	R2
70%	5	0.0238	10.87%	0.0318	0.9761
	10	0.0312	16.78%	0.0481	0.94
	20	0.0596	22.42%	0.0955	0.8788
90%	5	0.0094	2.50%	0.0129	0.9834
	10	0.0243	9.25%	0.0328	0.9818
	20	0.0390	9.95%	0.0733	0.8157

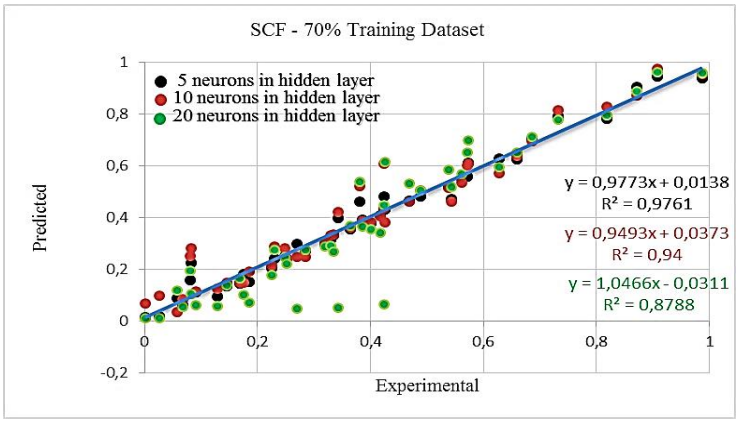

Fig. 6. 70% training dataset used ANN models.

The blue line represents the experimental (real) data, while the hidden layer's black, red, and green dots indicate 5-10-20 neurons in *Fig. 6* and *Fig. 7*, respectively. The prediction performances of three

constructed ANN models are calculated using linear regression analysis and mean square errors. It is clear that the prediction performance of the ANN model, which includes five neurons and is trained with both 70% and 90% of the dataset, produces the most realistic and effective results based on the SCF value.

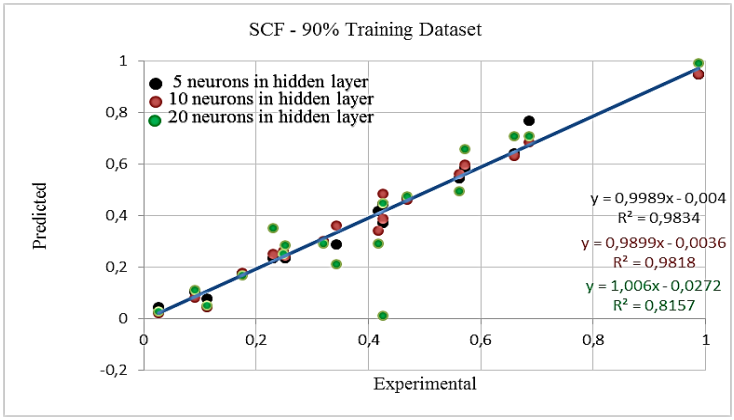

Fig. 7. %90 training dataset used ANN models.

5 | Conclusions

For more reliable welding operations, there should be no defects in the welding seams or within an acceptable range in welded constructions. The undercut is one of the most common welding flaws found on workpieces generated by butt welding. When the SCF value is determined, it is possible to decide whether to accept welding flaws in the case. SCF is influenced by a wide variety of parameters and their ranges, making it difficult to calculate a more precise SCF. Due to the many costs and limits of experiments, including the necessity for qualified personnel, repeat studies are extremely challenging. Traditional models struggle to address problems with such a complex structure. Thus, ANN is frequently used in modeling complex systems, providing good estimate performance between prediction models.

In this study, considering the calculation complexity of SCF, six ANN models are developed that differ in terms of the number of neurons in the hidden layer and the percentage of the training dataset. 6 ANN models, which include three input layers (Undercut depth (h) / Undercut deep Radius (r)), reinforcement angle (Q1), and deep angle of welding seam (Q2), a hidden layer which included three different numbers of neurons (5-10-20) and an output layer as SCF. 70% and 90% of the dataset is used for the training process of ANN models. Prediction performances of 6 developed ANN models are compared statistically. The best prediction performance is obtained with the 90% training dataset and five neurons in the hidden layer (R^2=0.9834). This value demonstrates that the SCF value may be obtained with good estimation performance without the requirement for experimentation and with a more cost- and time-effective use of laboratory resources. However, it is possible to determine the result of even a minor modification rapidly and accurately in any parameter. The two developed ANN models, which include five neurons in the hidden layer, are trained with 70% and 90% training datasets and are most effective in predicting SCF value. The increasing number of neurons in the hidden layer is found to have a negative impact on the prediction performance of ANN models. Therefore, studies can be made on the optimum number of neurons in the hidden layer between 5-10.

Compared to numerical and experimental studies, there are few studies on welding prediction models. It is crucial to thoroughly evaluate the situation and build the properly ANN model while building a prediction model. Good results are likely to be attained with a properly built model, saving time on experiments. The findings of the current study support that, in contrast to previous estimation studies for using specific parameter values, high estimation accuracy may be achieved by using all parameter values. The resulting predictions and the numerical experiment results are in good agreement with

testing examples, indicating the remarkable performance of ANN in the prediction of SCF of butt welding. Finally, numerous quantitative evaluations based on statistical error types validate the accuracy and effectiveness of the presented ANN predicting method.

The findings of this study enable effective welding error reduction without the need for experimentation. It makes suggestions for the research to be conducted in increasing job safety so that a useful result can be obtained in less time and at a lower cost. It should be mentioned that the model of this study is only applicable for variables that affect SCF. However, the proposed approach also provides a workable framework for additional problems. Machine learning techniques could also be employed with many parameters and experiments in future works.

References

[1] Terán, G., Albiter, A., & Cuamatzi-Meléndez, R. (2013). Parametric evaluation of the stress concentration factors in T-butt welded connections. *Engineering structures*, *56*, 1484–1495. https://doi.org/10.1016/j.engstruct.2013.06.031

[2] Holmstrand, T., Mrdjanov, N., Barsoum, Z., & Åstrand, E. (2014). Fatigue life assessment of improved joints welded with alternative welding techniques. *Engineering failure analysis*, *42*, 10–21. https://doi.org/10.1016/j.engfailanal.2014.03.012

[3] Teng, T.-L., Fung, C.-P., & Chang, P.-H. (2002). Effect of weld geometry and residual stresses on fatigue in butt-welded joints. *International journal of pressure vessels and piping*, *79*(7), 467–482. https://doi.org/10.1016/S0308-0161(02)00060-1

[4] Dabiri, M., Ghafouri, M., Raftar, H. R. R., & Björk, T. (2017). Neural network-based assessment of the stress concentration factor in a T-welded joint. *Journal of constructional steel research*, *128*, 567–578. https://doi.org/10.1016/j.jcsr.2016.09.024

[5] Guo, Z., Chen, H., & Yao, G. (2022). Bayesian prediction of the stress concentration effect on high-strength wires with corrosion pits. *Engineering failure analysis*, *131*, 105827. https://doi.org/10.1016/j.engfailanal.2021.105827

[6] Abbasnia, A., Jafari, M., & Rohani, A. (2021). A novel method for estimation of stress concentration factor of central cutouts located in orthotropic plate. *Journal of the Brazilian society of mechanical sciences and engineering*, *43*(7), 348. https://doi.org/10.1007/s40430-021-03061-x

[7] Makki, M. M., Ahmed, B., & Chokri, B. (2018). Reliability prediction of the stress concentration factor using response surface method. *The international journal of advanced manufacturing technology*, *94*(1), 817–826. https://doi.org/10.1007/s00170-017-0910-0

[8] Li, R., Miao, C., & Yu, J. (2020). Effect of characteristic parameters of pitting on strength and stress concentration factor of cable steel wire. *Construction and building materials*, *240*, 117915. https://doi.org/10.1016/j.conbuildmat.2019.117915

[9] Wang, Y., Luo, Y., & Tsutsumi, S. (2020). Parametric formula for stress concentration factor of fillet weld joints with spline bead profile. *Materials*, *13*(20), 4639. https://doi.org/10.3390/ma13204639

[10] Jiang, Y., Yuan, K., & Cui, H. (2018). Prediction of stress concentration factor distribution for multi-planar tubular DT-joints under axial loads. *Marine structures*, *61*, 434–451. https://doi.org/10.1016/j.marstruc.2018.06.017

[11] Bajić, D., Momčilović, N., Maneski, T., Balać, M., Kozak, D., & Ćulafić, S. (2017). Numerical and experimental determination of stress concentration factor for a pipe branch model. *Tehnicki vjesnik - technical gazette*, *24*(3), 687–692. https://doi.org/10.17559/TV-20151126222916

[12] Wang, B., Zhao, W., Du, Y., Zhang, G., & Yang, Y. (2016). Prediction of fatigue stress concentration factor using extreme learning machine. *Computational materials science*, *125*, 136–145. https://doi.org/10.1016/j.commatsci.2016.08.035

[13] Ozkan, M. T., & Toktas, I. (2016). Determination of the stress concentration factor (Kt) in a rectangular plate with a hole under tensile stress using different methods. *Materials testing*, *58*(10), 839–847. https://doi.org/10.3139/120.110933

[14] Ji, J., Zhang, C., Kodikara, J., & Yang, S.-Q. (2015). Prediction of stress concentration factor of corrosion pits on buried pipes by least squares support vector machine. *Engineering failure analysis*, *55*, 131–138. https://doi.org/10.1016/j.engfailanal.2015.05.010

[15] Zappalorto, M., & Carraro, P. A. (2015). An engineering formula for the stress concentration factor of orthotropic composite plates. *Composites part B: engineering*, *68*, 51–58. https://doi.org/10.1016/j.compositesb.2014.08.020

[16] Darwish, F., Gharaibeh, M., & Tashtoush, G. (2012). A modified equation for the stress concentration factor in countersunk holes. *European journal of mechanics - A/solids*, *36*, 94–103. https://doi.org/10.1016/j.euromechsol.2012.02.014

[17] Cerit, M. (2013). Numerical investigation on torsional stress concentration factor at the semi elliptical corrosion pit. *Corrosion science*, *67*, 225–232. https://doi.org/10.1016/j.corsci.2012.10.028

[18] Cerit, M., Kokumer, O., & Genel, K. (2010). Stress concentration effects of undercut defect and reinforcement metal in butt welded joint. *Engineering failure analysis*, *17*(2), 571–578. https://doi.org/10.1016/j.engfailanal.2009.10.010

[19] Arola, D., & Williams, C. L. (2002). Estimating the fatigue stress concentration factor of machined surfaces. *International journal of fatigue*, *24*(9), 923–930. https://doi.org/10.1016/S0142-1123(02)00012-9

[20] Ida, K., & Uemura, T. (1996). Stress concentration factor formulae widely used in japan. *Fatigue & fracture of engineering materials & structures*, *19*(6), 779–786. https://doi.org/10.1111/j.1460-2695.1996.tb01322.x

[21] Chang, E., & Dover, W. D. (1996). Stress concentration factor parametric equations for tubular X and DT joints. *International journal of fatigue*, *18*(6), 363–387. https://doi.org/10.1016/0142-1123(96)00017-5

[22] Guagliano, M., Terranova, A., & Vergani, L. (1993). Theoretical and experimental study of the stress concentration factor in diesel engine crankshafts. *Journal of mechanical design*, *115*(1), 47–52. https://doi.org/10.1115/1.2919323

[23] Özcanli, Y., Kosovali Çavuş, F., & Beken, M. (2016). Comparison of mechanical properties and artificial neural networks modeling of PP/PET blends. *Acta physica polonica A*, *130*(1), 444–446. https://doi.org/10.12693/APhysPolA.130.444

[24] Jahangiri, M., Farrokhi, A., & Amirabadi, A. (2021). Designing novel ldo voltage regulator implementation on FPGA using neural network. *Journal of applied research on industrial engineering*, *8*(3), 205–212.

[25] Erdem, B., Kiraz, A., & Kökümer, O. (2010). *Prediction of stress concentration factor in welding seam with artificial neural networks* [presentation]. Proceedings of the 1st international symposium on computing in science & engineering, Kusadasi, Aydin, Turkey.

[26] Eberhart, R. C., & Dobbins, R. W. (1990). *Neural network PC tools: a practical guide* (First Edition.). San Diego: Academic Press.

[27] Fausett, L. V. (1993). *Fundamentals of neural networks: architectures, algorithms and applications*. Englewood Cliffs, NJ.

[28] Shukla, R., Khalilian, B., & Partouvi, S. (2021). Academic progress monitoring through neural network. *Big data and computing visions*, *1*(1), 1–6.

[29] Çolak, A. B. (2021). An experimental study on the comparative analysis of the effect of the number of data on the error rates of artificial neural networks. *International journal of energy research*, *45*(1), 478–500. https://doi.org/10.1002/er.5680

[30] Kong, Y., Owusu-Akomeah, M., Antwi, H. A., Hu, X., & Acheampong, P. (2019). Evaluation of the robusticity of mutual fund performance in Ghana using enhanced resilient backpropagation neural network (ERBPNN) and fast adaptive neural network classifier (FANNC). *Financial innovation*, *5*(1), 10. https://doi.org/10.1186/s40854-019-0125-5

[31] Ghaedi, A. M., & Vafaei, A. (2017). Applications of artificial neural networks for adsorption removal of dyes from aqueous solution: a review. *Advances in colloid and interface science*, *245*, 20–39. https://doi.org/10.1016/j.cis.2017.04.015